Diamond & Related Materials 18 (2009) 587–591

Contents lists available at ScienceDirect

Diamond & Related Materials

journal homepage: www.elsevier.com/locate/diamond

Fluorescent nanodiamonds for specifically targeted bioimaging: Application to the interaction of transferrin with transferrin receptor

Mao-Feng Weng [a,b,*], Su-Yu Chiang [a,*], Niann-Shiah Wang [b], Huan Niu [c]

[a] National Synchrotron Radiation Research Center, Hsinchu 30076, Taiwan
[b] Department of Applied Chemistry, National Chiao Tung University, Hsinchu 30010, Taiwan
[c] Nuclear Science and Technology Department center, National Tsing Hua University, Hsinchu 30013, Taiwan

ARTICLE INFO

Available online 13 July 2008

Keywords:
Nanodiamonds
Transferrin
Confocal fluorescence images
Fluorescence lifetime

ABSTRACT

Fluorescent nanodiamonds (FND) as specifically targeted probes to image the interactions of transferrins (Tf) with their receptors that were over-expressed on HeLa cells were studied in this work. The 100-nm diamonds were irradiated with a 2.5-MeV ion beam and thermally annealed to emit bright fluorescence in the region 550–800 nm upon excitation at 514.5 nm; accordingly, the interference of cellular autofluorescence at 520–650 nm was eliminated significantly on detecting fluorescence at >660 nm. FND-Tf bioconjugates were produced via the formation of an amide bond between carboxylated FND and transferrin and used to target transferrin receptors (TfR) on HeLa cells for activity testing. The receptor-mediated uptake of FND-Tf bioconjugates into HeLa cells was confirmed from confocal fluorescence images; in contrast, the uptake of FND-Tf bioconjugates on presaturated receptors or carboxylated FND on HeLa cells was unobserved. We measured also the fluorescence spectra and lifetimes of carboxylated FND, FND-Tf bioconjugates and FND-Tf–TfR complexes for characterization. Their measured lifetimes are 11.8 ± 0.1, 11.6 ± 0.1 and 12.1 ± 0.1 ns, respectively, and fluorescence spectra are comparable except that the two zero-phonon lines of FND-Tf–TfR complexes become indistinct. Both results show that the surface effects of chemical interactions on the emission center of FND are negligible.

1. Introduction

Fluorescent nanodiamonds (FND) as optical probes to image biological systems have attracted considerable attention because of their special optoelectronic properties — bright fluorescence, protracted photostability and a broad spectral range, as well as because of their low cytotoxicity and ease of conjugation with biomolecules after surface functionalization [1–12]. The bright fluorescence of nanodiamonds results from nitrogen-vacancy (N-V) centers that are created with high-energy electron or ion bombardment of type Ib nanodiamonds, followed by thermal annealing [1–3,13]. Fu et al. reported a minute effect on the photostability and brightness of fluorescence after a surface treatment and electrostatic interactions [3]. As the zero-phonon lines (ZPL) in fluorescence spectra and the fluorescence lifetimes of FND are expected to be sensitive to environmental changes, the surface effect can also be characterized on monitoring the variations of ZPL and lifetimes under different conditions [14–17].

Several methods of surface functionalization of nanodiamonds (ND) to interact with biomolecules via covalent bonding for further study of specific or non-specific interactions in biological systems have been reported [3,7,8,18,19]. The carboxylation of ND on treatment with strong oxidizing acid is a simple method to produce carboxylated FND (FND-COOH) that can react with biomolecules to form covalent amide bonds via carbodiimide chemistry [20,21]. A non-specific binding between the covalent bonding FND-poly-L-lysine bioconjugates and DNA molecules through electrostatic interactions was demonstrated to show the capability of FND as cell biomarkers [3], but the specific recognition of bioconjugates to graft the biologically active moieties is particularly important for applications, for example, in the examination of biochemical reactions and drug delivery [22–25]. Transferrin targets preferentially its receptor to form a strongly bound complex; moreover, the uptake of transferrin on HeLa cells is expected through the mediation of transferrin receptors that are over-expressed on the surfaces of HeLa cells [26,27]. The mediated uptake of transferrin on HeLa cells hence serves as an excellent case for the investigation of specific interactions.

In this work, we investigated the application of FND as specifically targeted fluorescence probes to image the interactions of transferrins with receptors that were over-expressed on HeLa cells with a laser-scanning fluorescence microscope. FND were produced on irradiation with a 2.5-MeV proton beam and thermal annealing before being functionalized with carboxyl groups to link to transferrin to form FND-Tf bioconjugates. The uptake of FND-Tf bioconjugates on a HeLa cell was confirmed, and two control experiments were performed to verify the uptake through a Tf–TfR interaction. We measured also the fluorescence spectra and fluorescence lifetimes of carboxylated FND, FND-Tf

* Corresponding authors. National Synchrotron Radiation Research Center, Hsinchu 30076, Taiwan.
E-mail addresses: mfweng@nsrrc.org.tw (M.-F. Weng), schiang@nsrrc.org.tw (S.-Y. Chiang).

0925-9635/$ – see front matter © 2008 Elsevier B.V. All rights reserved.
doi:10.1016/j.diamond.2008.07.012

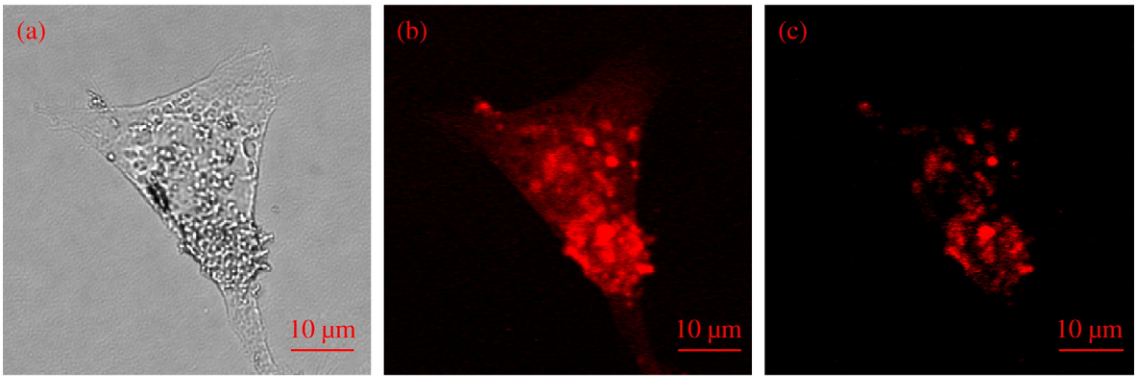

Fig. 1. Images of a fixed HeLa cell after treatment with FND-Tf bioconjugates (10 μg/mL) for 1 h in an incubator; (a) bright-field image, (b) confocal scanning image obtained on collecting fluorescence of FND at >550 nm upon excitation at 514.5 nm; (c) confocal scanning image with fluorescence collected at 663–738 nm. Each image was obtained with a 60× objective in a field of view 60×60 μm^2.

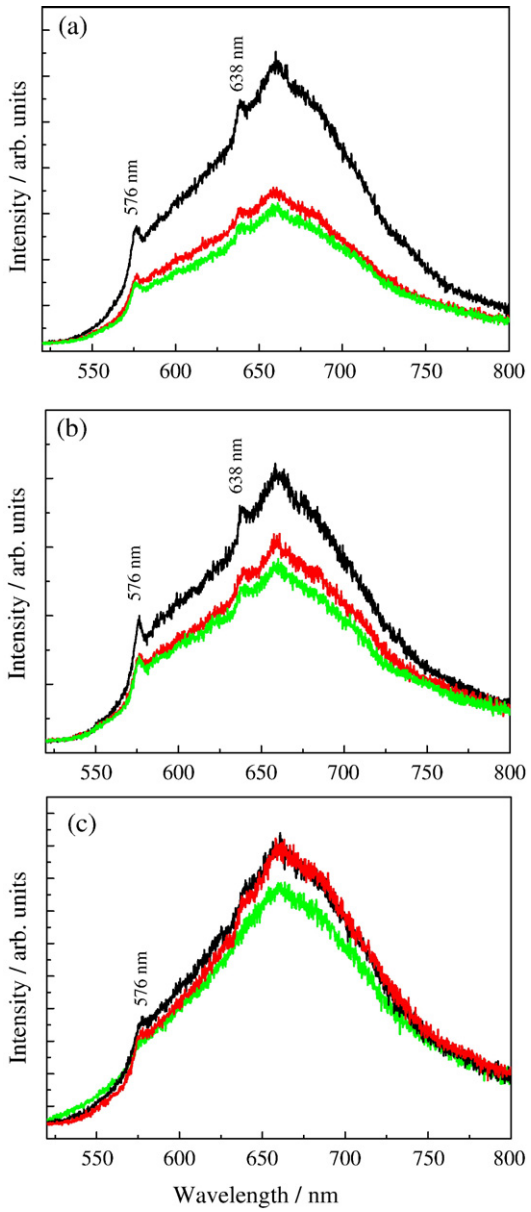

Fig. 2. Comparison of fluorescence spectra of (a) carboxylated FND, (b) FND-Tf bioconjugates, and (c) FND-Tf–TfR complexes on a fixed HeLa cell; the three spectra in each figure were obtained from separate locations; their intensity variations are due mainly to variability in the number of N-V centers of FND.

bioconjugates and FND-Tf–TfR complexes to understand the surface effects due to the chemical interactions.

2. Experiments

Synthetic type Ib nanodiamonds of average diameter 100 nm (Micron+MDA, Element Six) served as targeted fluorescence probes

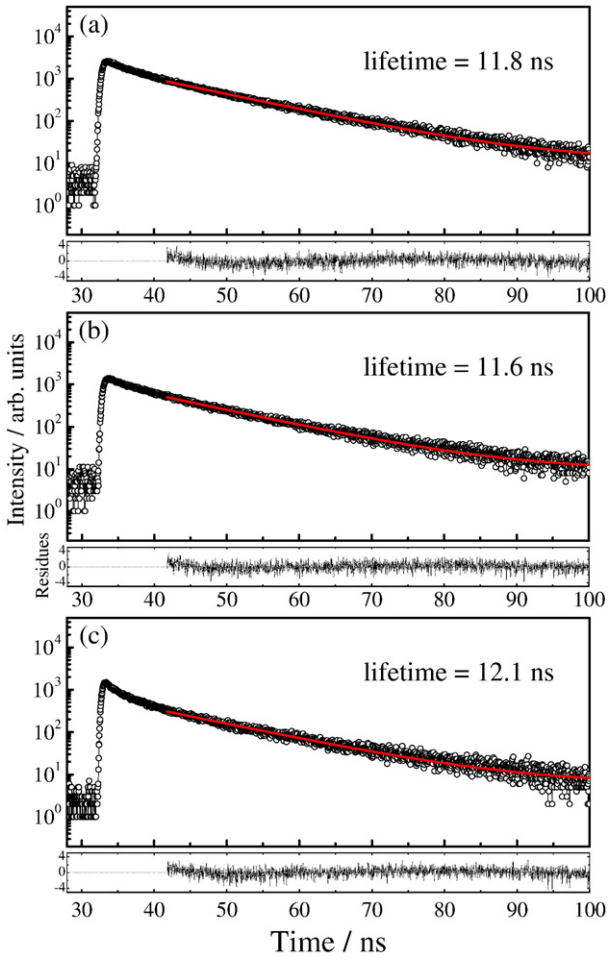

Fig. 3. Fluorescence lifetime curves of FND in the form of (a) carboxylated FND, (b) FND-Tf bioconjugates, and (c) FND-Tf–TfR complexes on a fixed HeLa cell with signals collected at 663–738 nm; a single exponential-decay curve is fitted to the selected data after background subtraction and the resultant curve with background included is plotted as a red solid line with residues shown below. (For interpretation of the references to color in this figure legend, the reader is referred to the web version of this article.)

after proton-beam irradiation and thermal annealing according to published reports [2,3,17]. The 2.5-MeV proton beam source with beam current 0.8 μA (KN, High Voltage) is located at the accelerator laboratory of National Tsing Hua University in Taiwan. Typically, a nanodiamond film (depositing a nanodiamond solution 50 μL, concentration 10 mg/mL) was irradiated 30 min with the proton beam at a dose 1.6×10^{16} protons/cm^2 to create sufficient nitrogen-vacancy (N-V) centers. Subsequent thermal annealing of the irradiated nanodiamond film in vacuum at 800 °C for 2 h facilitates the formation of negatively charged nitrogen-vacancy (N-V$^-$) centers from which bright fluorescence is emitted upon excitation at 514.5 nm. The produced FND were cleaned and surface-functionalized to form carboxylated FND according to a treatment with strong oxidizing acid [6]; FND were first immersed in a mixture of concentrated H_2SO_4 and HNO_3 with a volume ratio ~9 at 25 °C for 24 h, then in NaOH aqueous solution (0.1 M) at 90 °C for 2 h, and finally in HCl aqueous solution (0.1 M) at 90 °C for 2 h. For formation of FND-Tf bioconjugates, transferrin (MW~80 kDa; T4382, Sigma, 0.1 mg) and carboxylated FND (0.2 mg) were incubated in phosphate buffer saline (PBS, 1 mL, pH=7.4) at 25 °C for 24 h, with an addition of *N*-(3-dimethylaminopropyl)-*N′*-ethyl-carbodiimide hydrochloride (E7750, Sigma, 5 mg) to activate the reaction. The FND-Tf bioconjugates produced were then purified through a cycle – separation by sedimentation with a centrifuge and suspension in PBS buffer – three times before use. In the uptake experiments, FND-Tf bioconjugates in PBS buffer were added to the culture media of HeLa cells (final concentration 10 μg/mL) and incubated (37 °C) in an incubator (5% CO_2) for 1 h. HeLa cells were cultured in DMEM (Invitrogen) supplemented with fetal bovine serum (FBS, 10%) and penicillin/streptomycin (1%) for incubation (12 h) before treatment; moreover, as cell aggregations at ~10^5 cells/mL were observed after 12 h incubation, ~10^4 cells/mL in the experiments were used to obtain superior cell morphology. The treated HeLa cells were washed several times with PBS buffer and fixed to a cover-glass plate with paraformaldehyde (Sigma, 4%) for fluorescence measurements. Of two control experiments to confirm that receptor-mediated uptake of FND-Tf bioconjugates into HeLa cells occurs exclusively, one is with cells treated with carboxylated FND (final concentration 10 μg/mL) with incubation (1 h), and the other is with HeLa cells presaturated with free transferrin (1 mg/mL) with incubation (1 h) before treatment with FND-Tf bioconjugates.

Confocal fluorescence images were measured on an inverted microscope (TE2000, Nikon) equipped with a scanning head (C1, Nikon)

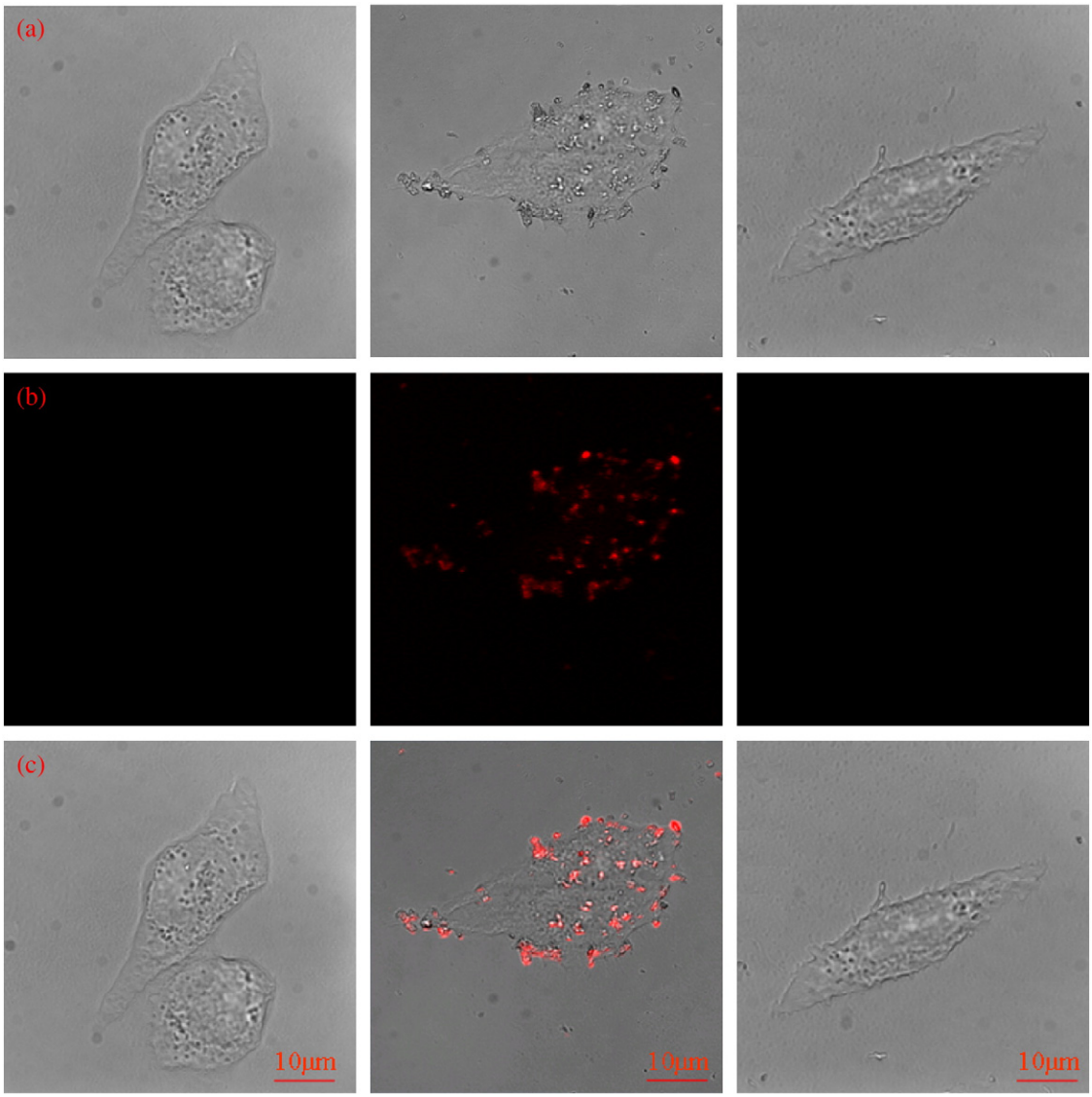

Fig. 4. Comparison of confocal fluorescence images of HeLa cells treated with carboxylated FND and FND-Tf bioconjugates; (a) the left two bright-field images are HeLa cells treated respectively with carboxylated FNDs and FND-Tf bioconjugates, and the right one image is a HeLa cell presaturated with free transferrin for 1 h before being treated with FND-Tf bioconjugates; (b) corresponding confocal fluorescence images obtained upon excitation at 514.5 nm; (c) overlays of bright and fluorescence images.

and an Ar-ion laser (210AL, National Laser). The 514.5-nm laser line (20 μW) was focused through a water immersion objective (60×, NA 1.2, Nikon) onto the sample and the fluorescence was collected with the same objective, passed through a band-pass filter (ET700/75 m-2p, Chroma Tech) and a pinhole (diameter 60 μm) before being detected with a photomultiplier. For measurements of fluorescence spectra, fluorescence was focused into a spectrometer (Triax 320, Jobin-Yvon, 0.32 m) before detection; spectra in a region 520–800 nm were recorded at a step 0.2 nm and with an acquisition period 1 s. For lifetime measurements, a 470 nm diode laser (PicoQuant) operated at 10 MHz was used as the excitation light source and fluorescence was detected with an APD (SPCM-AQR-14-FC, Perkin-Elmer) before being transferred to a time-correlated single photon counting module (TimeHarp200, PicoQuant) for further processing.

3. Results and discussion

The strong fluorescence spectrum of FND in a region 550–800 nm with a maximum at ~660 nm had two ZPL at 576 and 638 nm upon excitation at 514.5 nm, consistent with previous reports with 3-MeV proton-beam irradiation [3,17]; the ZPL are attributed to electronic transitions of neutral nitrogen-vacancy centers $(N\text{-}V)^0$ and negatively charged defect centers $(N\text{-}V)^-$, respectively [3,13,28,29]. As the fluorescence maximum at ~660 nm is separate from the autofluorescence of a HeLa cell in a region 520–650 nm, we collected the fluorescence of FND in a region 663–738 nm to eliminate the interference of HeLa cell autofluorescence for imaging. The diminution of HeLa cell autofluorescence on taking advantage of strong fluorescence in the long-wavelength region is demonstrated in Fig. 1. Fig. 1(a) presents a bright-field image of a fixed HeLa cell after being treated with FND-Tf bioconjugates (final concentration 10 μg/mL) for 1 h in an incubator; the field of view is 60×60 μm^2. The corresponding confocal fluorescence images obtained on collecting fluorescence of FND at >550 nm and in a region 663–738 nm upon excitation at 514.5 nm are shown in Fig. 1(b) and (c) to demonstrate the differentiation.

Fig. 2 (a)–(c) shows a comparison of fluorescence spectra of carboxylated FND, FND-Tf bioconjugates and FND-Tf–TfR complexes on HeLa cells, respectively; the three spectra for each species were obtained from three separate locations to show the intensity variations, resulting mainly from a variation in the numbers of N-V center of FND. As seen in Fig. 2, there is no significant difference in these spectra, except that two ZPL in the FND-Tf–TfR complexes become indistinct, likely due to the heterogeneous environments of HeLa cells as it is commonly observed in solid-state chemistry that ZPL were obscured by strong phonon sidebands that result mainly from disordered lattice structures [30–32].

To understand the effect of environmental changes, we measured also the fluorescence lifetimes of FND in the three complexes. Fig. 3 (a)–(c) shows the measured fluorescence lifetime curves of carboxylated FND, FND-Tf bioconjugates and FND-Tf–TfR complexes on HeLa cells; a single exponential-decay curve is fitted to the selected data after background subtraction for each species and a resultant curve

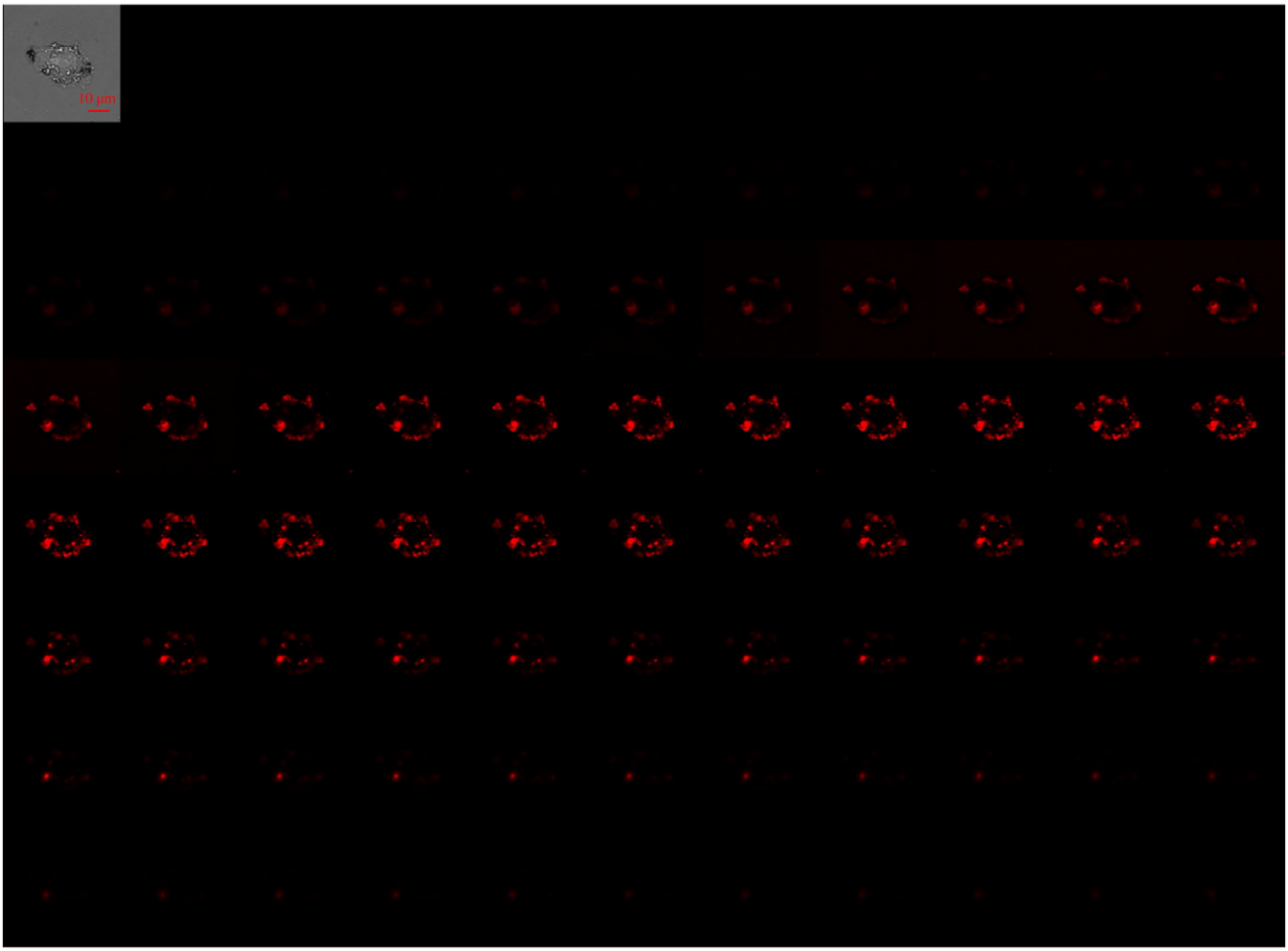

Fig. 5. Confocal fluorescence images of a HeLa cell treated with FND-Tf bioconjugates, recorded with a step 200 nm in the vertical direction and presented from left to right and top to bottom with a field of view 60×60 μm^2 for each image.

with background included is plotted as a red solid line with residues shown below. The measured lifetimes for these three complexes are 11.8 ± 0.1, 11.6 ± 0.1 and 12.1 ± 0.1 ns, respectively. Although the fluorescence lifetime is expected to be sensitive to environmental change, small but insignificant differences resulting from the Tf–TfR interaction on HeLa cell were observed. These results together with the nearly identical spectra indicate that the surface effects of chemical interactions on the emission center of FND are negligible; the cause is ascribed to the N-V centers embedded in the crystal lattice, as mentioned by Fu et al. who found that the fluorescence intensity of FND before and after treatment with strong oxidizing acids is nearly the same [3].

Fig. 4 shows a comparison of the confocal fluorescence images of fixed HeLa cells treated respectively with carboxylated FND and FND-Tf bioconjugates to demonstrate the specific biorecognition function of FND-Tf bioconjugates. In Fig. 4(a), the left two bright-field images are HeLa cells treated respectively with carboxylated FNDs and FND-Tf bioconjugates, and the right one image is a HeLa cell presaturated with free transferrin for 1 h before being treated with FND-Tf bioconjugates; the field of view is 60 × 60 μm^2 for each image. Fig. 4(b) shows the corresponding confocal fluorescence images obtained upon excitation at 514.5 nm; Fig. 4(c) shows overlays of fluorescence and the corresponding transmission images to illustrate the distributions of FND-bioconjugates within HeLa cells.

In the left panel of Fig. 4(b), the absence of fluorescence signals reflects no carboxylated FND binding to HeLa cells as the unbound carboxylated FND were washed away with PBS buffer. This result demonstrates that the interference of non-specific interactions originating from carboxylated FND is negligible — an advantage to facilitate the recognition of specific interactions. Moreover, the lack of non-specific binding for 100-nm carboxylated FND is contrary to the translocation of 35-nm FND through membrane of a HeLa cell reported previously [3]; the discrepancy might be caused by the size difference, but detailed studies to understand the size effect are required. In the middle panel of Fig. 4(b), the uptake of FND-Tf bioconjugates into the HeLa cell was confirmed according to the aggregates observed inside the cell. The lack of fluorescence image in the control experiment of HeLa cells presaturated with free transferrin to block the available receptors before being treated with FND-Tf bioconjugates, shown in the right panel of Fig. 4(b), further confirms the uptake of FND-Tf bioconjugates through specific Tf–TfR interactions. These results also demonstrate that the 100-nm FND did not block the active site of transferrin for receptor binding although its size is over ten times that of transferrin; moreover, the distinctive boundary of the HeLa cell after the uptake of FND-Tf bioconjugates shown in the figure indicates a small cytotoxicity of FND, an important advantage for applications of FND in biological system.

An issue regarding the transport of FND-Tf bioconjugates into HeLa cells through receptor-mediated endocytosis, a common ion transport occurring in cells [26,27], was examined on recording the confocal fluorescence images of the HeLa cell at varied depths. Fig. 5 shows vertical cross-sectional confocal fluorescence images of a HeLa cell treated with FND-Tf bioconjugates presented in an order from left to right and top to bottom; the field of view for each image is 60 × 60 μm^2. As seen in Fig. 5, FND shown as red spots were observed within a thickness ~ 10 μm, indicative of translocation of FND through the cell membrane. In contrast, fluorescence images inside the cell were unobserved in the two control experiments, reflecting no translocation of the carboxylated FND and FND-Tf bioconjugates due mostly to a lack of specific Tf–TfR interactions. Hence, we conclude that the FND-Tf–TfR complexes originally formed on the surface of a HeLa cell through Tf–TfR interactions were engulfed by the cell, likely through an endocytosis pathway.

4. Conclusion

We demonstrated the application of FND as targeted fluorescence probes to investigate the interactions of transferrins and their receptors on HeLa cells. The uptake of FND-Tf bioconjugates into a HeLa cell via a specific Tf–TfR interaction is verified based on confocal fluorescence images; two control experiments, one with an uptake of carboxylated FND and the other with HeLa cells presaturated with free transferrins before addition of FND-Tf bioconjugates, were performed to confirm the specifically targeted function of FND-Tf bioconjugates. We measured also the fluorescence spectra and lifetimes of FND in the forms of carboxylated FND, FND-Tf bioconjugates and FND-Tf–TfR complexes on the HeLa cell; the nearly identical spectra and the measured lifetimes near 11.8 ns for all three complexes indicate a negligible surface effect caused by chemical interactions. That FND provide advantages – strong fluorescence in the long-wavelength region, ease of surface functionalization for specifically targeted imaging and a negligible surface effect – was demonstrated in this work.

Acknowledgments

This work was supported by grants from National Synchrotron Radiation Research Center (NSRRC) and National Science Council (NSC) of Taiwan (Contract No. NSC96-2113-M-213-005-MY2). We thank Dr. Po-Long Wu at NSRRC for helping us on the preparation of HeLa cells.

References

[1] A. Gruber, A. Drabenstedt, C. Tietz, L. Fleury, J. Wrachtrup, C. von Borczyskowski, Science 276 (1997) 2012.
[2] S.J. Yu, M.W. Kang, H.C. Chang, K.M. Chen, Y.C. Yu, J. Am. Chem. Soc. 127 (2005) 17604.
[3] C. Fu, H.Y. Lee, K. Chen, T.S. Lim, H.Y. Wu, P.K. Lin, P.K. Wei, P.H. Tsao, H.C. Chang, W. Fann, PNAS 104 (2007) 727.
[4] A.M. Schrand, H. Huang, C. Carlson, J.J. Schlager, E. Osawa, S.M. Hussain, L. Dai, J. Phys. Chem. B 111 (2007) 2.
[5] L.C.L. Huang, H.C. Chang, Langmuir 20 (2004) 5879.
[6] X.L. Kong, L.C.L. Huang, C.M. Hsu, W.H. Chen, C.C. Han, H.C. Chang, Anal. Chem. 77 (2005) 259.
[7] A. Kruger, Angew. Chem. Int. Ed. 45 (2006) 6426.
[8] A. Kruger, Y. Liang, G. Jarre, J. Stegk, J. Mater. Chem. 16 (2006) 2322.
[9] Y.L. Zhenning, G. John, L. Margrave, V.N. Khabashesku, Chem. Mater. 16 (2004) 3924.
[10] K.K. Liu, C.L. Cheng, C.C. Chang, J.I. Chao, Nanotechnology 18 (2007) 325102.
[11] E. Perevedentseva, C.Y. Cheng, P.H. Chung, J.S. Tu, Y.H. Hsieh, C.L. Cheng, Nanotechnology 18 (2007) 315102.
[12] B.R. Smith, M. Niebert, T. Plakhotnik, A.V. Zvyagin, J. Lumin. 127 (2007) 260.
[13] J.E. Field, The Properties of Natural and Synthetic Diamond, Academic Press, New York, 1992.
[14] H. Nishikori, Y. Mita, Y. Nisida, M. Okada, T. Nakashima, Phys. Stat. Sol. (c) 4 (2007) 1122.
[15] I. Favero, A. Berthelot, G. Cassabois, C. Voisin, C. Delalande, P. Roussignol, R. Ferreira, J.M. Gerard, Phys. Rev. B 75 (2007) 073308.
[16] W. Becker, A. Bergmann, E. Haustein, Z. Petrasek, P. Schwille, C. Biskup, L. Kelbauskas, K. Benndorf, N. Klocker, T. Anhut, I. Riemann, K. Konig, Microsc. Res. Tech. 69 (2006) 186.
[17] T.L. Wee, Y.K. Tzeng, C.C. Han, H.C. Chang, W. Fann, J.H. Hsu, K.M. Chen, Y.C. Yu, J. Phys. Chem. A 111 (2007) 9379.
[18] A. Krueger, Chem. Eur. J. 14 (2008) 1382.
[19] C.Y. Cheng, E. Perevedentseva, J.S. Tu, P.H. Chung, C.L. Cheng, K.K. Liu, J.I. Chao, P.H. Chen, C.C. Chang, Appl. Phys. Lett. 90 (2007) 163903.
[20] Y.S. Lin, P.J. Tsai, M.F. Weng, Y.C. Chen, Anal. Chem. 77 (2005) 1753.
[21] G.T. Hermanson, Bioconjugate Techniques, Academic Press, New York, 1996.
[22] I.Z.R. Mendez, Y. Shi, H. HogenEsch, S.L. Hem, Vaccine 25 (2007) 825.
[23] P. Bajcsy, S.C. Lee, A. Lin, R. Folberg, J. Microsc. 221 (2006) 30.
[24] M. Dziedzicka-Wasylewska, A. Faron-Gorecka, J. Andrecka, A. Polit, M. Kusmider, Z. Wasylewski, Biochemistry, 45 (2006) 8751.
[25] F. Waharte, C. Spriet, L. Heliot, Cytom. Part A 69A (2006) 299.
[26] T.R. Daniels, T. Delgado, J.A. Rodriguez, G. Helguera, M.L. Penichet, Clin. Immunol. 121 (2006) 144.
[27] T.R. Daniels, T. Delgado, J.A. Rodriguez, G. Helguera, M.L. Penichet, Clin. Immunol. 121 (2006) 159.
[28] N.B. Manson, J.P. Harrison, M.J. Sellars, Phys. Rev. B 74 (2006) 104303.
[29] F. Treussart, V. Jacques, E. Wu, T. Gacoin, P. Grangier, J.F. Roch, Physica B 376–377 (2006) 926.
[30] S. Hayama, G. Davies, J. Tan, J. Coutinho, R. Jones, K.M. Itoh, Phys. Rev. B 70 (2004) 035202.
[31] L. Bergman, M.T. Mcclure, J.T. Glass, R.J. Nemanich, J. Appl. Phys. 76 (1994) 3020.
[32] J. Friedrich, D. Haarer, Angew. Chem. Int. Ed. 23 (1984) 113.